

## Enhancing single-parameter quantum charge pumping in carbon-based devices

Luis E. F. Foa Torres,<sup>1,a)</sup> Hernán L. Calvo,<sup>1,2</sup> Claudia G. Rocha,<sup>3,4</sup> and Gianaurelio Cuniberti<sup>4,5</sup>

<sup>1</sup>*Instituto de Física Enrique Gaviola (IFEG-CONICET) and FaMAF, Universidad Nacional de Córdoba, Ciudad Universitaria, Córdoba 5000, Argentina*

<sup>2</sup>*Institut für Theorie der Statistischen Physik, RWTH Aachen University, Aachen D-52056, Germany*

<sup>3</sup>*Department of Physics, NanoScience Center, University of Jyväskylä, Jyväskylä 40014, Finland*

<sup>4</sup>*Institute for Materials Science and Max Bergmann Center of Biomaterials, Dresden University of Technology, Dresden D-01062, Germany*

<sup>5</sup>*Division of IT Convergence Engineering, POSTECH, Pohang 790-784, South Korea*

(Received 15 July 2011; accepted 8 August 2011; published online 29 August 2011)

We present a theoretical study of quantum charge pumping with a single ac gate applied to graphene nanoribbons and carbon nanotubes operating with low resistance contacts. By combining Floquet theory with Green's function formalism, we show that the pumped current can be tuned and enhanced by up to two orders of magnitude by an appropriate choice of device length, gate voltage intensity, and driving frequency and amplitude. These results offer a promising alternative for enhancing the pumped currents in these carbon-based devices. © 2011 American Institute of Physics. [doi:10.1063/1.3630025]

A current flow in a two terminal conductor normally requires a bias voltage difference between the electrodes. However, in systems where the coherence length of the electrons exceeds the device length, the use of ac fields can produce a non-vanishing current even at zero bias voltage. This quantum coherent effect is called *quantum charge pumping*<sup>1–3</sup> and has been observed experimentally.<sup>4–6</sup> When the driving frequency ( $\Omega$ ) is low enough in such a way that  $\Omega \ll \tau^{-1}$  (being  $\tau$  the time spent by an electron to traverse the sample) then the transport is said to be adiabatic. Under such conditions, at least two out of phase time-dependent parameters are necessary to achieve pumping.<sup>7</sup> Beyond the realm of the adiabatic approximation, pumping with a single parameter is also possible<sup>8–12</sup> as confirmed by recent experiments.<sup>13–15</sup> While a drawback for such monoparametric pumps is that higher frequencies are required to achieve similar currents, a big advantage comes from the reduction in the number of necessary contacts which makes it promising for scalable, low-dissipation, devices. In this way, single-parameter pumping has become a quest for achieving higher currents in nanoscale transmission channels.

The advent of graphene<sup>16</sup> and their lower dimensional cousins, graphene nanoribbons, and carbon nanotubes,<sup>17</sup> provided an outstanding ground for exploring the physics of quantum charge pumping as evidenced by recent studies. Most of them are focused in flat graphene samples driven in the adiabatic regime<sup>18–20</sup> or beyond the adiabatic regime but in the energy range close to the Dirac point.<sup>21,22</sup> The observation of other prominent features such as van Hove singularities (vHS) usually requires an important gate voltage but recent experiments performed on twisted graphene layers demonstrate that singularities can be brought arbitrarily close to the Fermi energy,<sup>23</sup> opening interesting prospects for beyond-the-Dirac-point-studies.

In this letter, we explore the interplay between electronic structure and non-adiabatic effects in carbon-based quantum pumping devices with a *single* parameter. The transmission channels are composed of carbon nanotubes or graphene nanoribbons but our results are expected to be valid for generic quasi one-dimensional systems. By modeling a device with low resistance contacts and driven by a single time-dependent gate, we show that the pumped current can be enhanced by up to two orders of magnitude by gating the system close to a van Hove singularity. Moreover, it is shown that substantial improvement is also possible at the Dirac point when tuning the interplay between driving frequency and device length. Our study points out alternative directions to bring these devices closer to reality.

*Tight-binding model and Floquet solution.* We consider a device consisting of a graphene nanoribbon with passivated edges, or a single wall carbon nanotube, of length  $L$  connected to two semi-infinite electrodes. For the sake of simplicity, the electrodes are considered to be a prolongation of the sample located at the centre. The system is described through a single  $\pi$ -orbital Hamiltonian<sup>17</sup>  $H_e = \sum_i E_i c_i^\dagger c_i - \sum_{\langle i,j \rangle} [\gamma_{i,j} c_i^\dagger c_j + \text{H.c.}]$ , where  $c_i^\dagger$  and  $c_i$  are the creation and annihilation operators for electrons at site  $i$ ,  $E_i$  are the on site energies and  $\gamma_{i,j}$  are nearest-neighbors carbon-carbon hoppings. To simulate a system with low resistance contacts, the central part of length  $L$  (the “sample”) is connected to the semi-infinite leads through matrix elements  $\gamma_t$ , the carbon-carbon hopping<sup>24</sup>  $\gamma = 2.7$  eV.<sup>17</sup> We set  $\gamma_t = 0.7\gamma$  in order to mimic the Fabry-Perot conductance oscillations,<sup>25</sup> experimentally observed at low temperatures.<sup>26</sup>

In addition to the possibility of homogeneously gating the whole central sample, which is useful for revealing Fabry-Perot oscillations as in Ref. 26, here, we include an ac gate asymmetrically disposed on the scattering region as represented at the bottom of Fig. 1. The ac gate, which is responsible for the dynamical breaking of the left-right symmetry, is modelled through an additional on site energy

<sup>a)</sup>Author to whom correspondence should be addressed. Electronic mail: lfoa@famaf.unc.edu.ar.

term  $E_{j \in G} = eV_{ac} \cos(\Omega t) + eV_{gate}$  where  $G$  is the region where the ac gate is applied,  $V_{ac}$  is the amplitude of the ac gate,  $V_{gate}$  is the one of a static gate which is applied to the whole sample, and  $\Omega$  is the driven frequency. The current is obtained by using Floquet theory.<sup>9,27,28</sup> The dc component of the time-dependent current  $I(t)$  can be computed as

$$\bar{I} = \frac{2e^2}{h} \sum_n \int [T_{R \rightarrow L}^{(n)}(\varepsilon) f_L(\varepsilon) - T_{L \rightarrow R}^{(n)}(\varepsilon) f_R(\varepsilon)] d\varepsilon, \quad (1)$$

where  $T_{R \rightarrow L}^{(n)}(\varepsilon)$  are the transmission probabilities of the carriers coming from the left (L) to right (R) electrodes which might absorb or emit  $|n|$  photons depending if  $n > 0$  or  $n < 0$ , respectively. These transmission probabilities can be fully written in terms of the Floquet Green's functions for the system as explained in Ref. 11. The number of Floquet channels ( $n$ ) used in the calculation is chosen by requiring the convergence of the transmission functions with at least six significant digits. The electron distribution in the left (right) lead is given by the Fermi function  $f_L(\varepsilon)$  ( $f_R(\varepsilon)$ ). The non-interacting model is justified when screening by the surrounding gate or a metallic substrate reduces electron-electron interactions, ruling out effects beyond our present scope.<sup>29</sup> At the same time, electron-phonon interactions can be ruled out at low bias voltages ( $< 150$  meV) since the relevant inelastic mean free path for scattering with acoustical phonons is on the order of 1-2 micrometers at 300 K.<sup>30</sup> Recently, a similar method was applied to unveil laser-induced band gaps in graphene and their effect on charge transport.<sup>31</sup>

*Single-parameter pumping: interplay between electronic structure and non-adiabatic effects.* Although in the following we present results for metallic nanotubes, the same physics was found for armchair edge graphene nanoribbons. This is consistent with the argument proposed in Ref. 32 based on the use of a mode decomposition scheme for the electronic states. Furthermore, we expect the trends found here to be valid for a

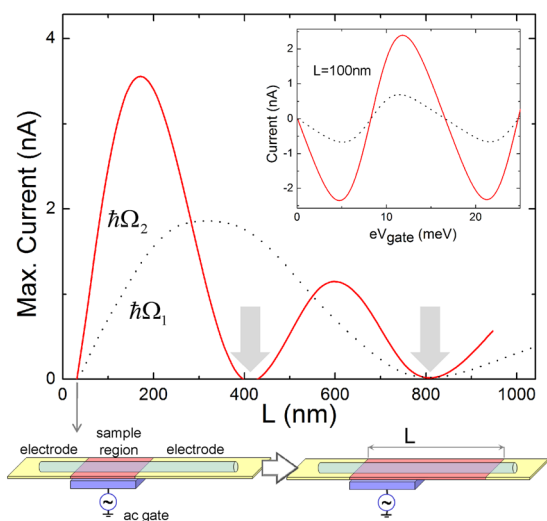


FIG. 1. (Color online) Inset: Pumped current as a function of the gate voltage for a (24, 0) carbon nanotube with  $L = 100$  nm. Main frame: maximum current pumping as a function of the system length at two fixed driven frequencies: (solid red line)  $\hbar\Omega_2 = 4.050$  meV and (dotted line)  $\hbar\Omega_1 = 2.025$  meV. The ac field intensity is set to  $eV_{ac} = 1.35$  meV. The vertical down arrows (grey) mark the points where the pumped current vanishes. Bottom panels: schematic representation of the system with symmetric (left) and asymmetric (right) ac gate.

generic quasi one-dimensional system. Figures 1 and 2 show the maximum pumped current calculated for a (24, 0) carbon nanotube with an asymmetrical ac gate (see bottom schemes in Fig. 1) extending over a typical length  $L_{ac} = 30$  nm.

When pumping close to the charge neutrality point (CNP), the Fabry-Perot oscillations manifest as an oscillatory pumped current as shown in the inset of Fig. 1. Its period is the energy level spacing,  $\Delta$ , which characterizes the system spectrum. Changing the device length allows the tuning of  $\Delta \propto 1/L$ . On Fig. 1 (main frame), one can notice that the maximum pumped current can be strongly modulated by the device length. The solid red line corresponds to a driving frequency which doubles the one for the dotted line. The zeroes in these curves (marked with down arrows) can be understood in terms of a *wagon-wheel effect*:<sup>32,33</sup> whenever the driving frequency is commensurate with the level spacing, the system behaves as in the static case and no current is pumped. A similar phenomenon was noted in Ref. 9 for a double barrier structure. Another feature is the decrease of the successive maxima in Fig. 1 (main frame). To explain this issue, first, one notes that the pumped current is obtained by integrating a kernel function given in Eq. (1), which in our case turns out to be periodic as demonstrated on Fig. 1 inset. While the kernel amplitude remains approximately constant when changing the device length, the relevant energy scale over which the integration is performed is  $\min(\hbar\Omega, \Delta)$ . This leads for big enough  $L$  to a series of maxima which scale with  $\Delta \propto 1/L$  as seen in Fig. 1 (main frame).

Beyond the CNP, application of a gate voltage can unveil interesting features when tuned nearby vHS. The physics in this case becomes more transparent if the total current is split into the contributions due to the different subbands. This is achieved by resorting to a unitary transformation which diagonalizes the electronic Hamiltonian for each layer perpendicular to the transport direction.<sup>34</sup> For a  $(N, 0)$  nanotube, the different subbands correspond to linear chains with

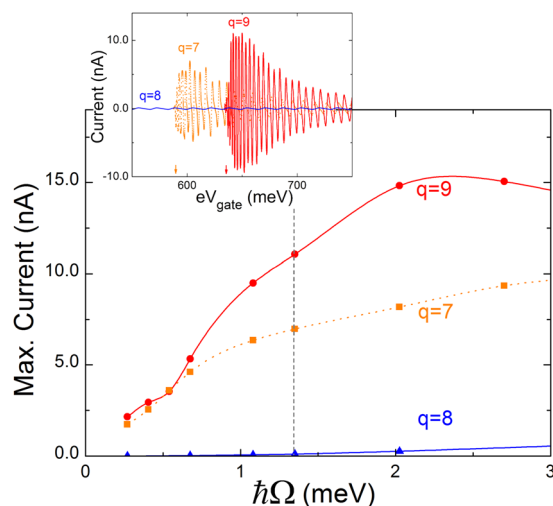


FIG. 2. (Color online) Maximum current pumping obtained for (24,0) carbon nanotube. Inset: Pumped current as a function of the gate voltage. The different curves are the contributions from the different sub-bands. The position of the van Hove singularities is indicated with arrows on the horizontal axis. The driving frequency used in the inset is marked with a vertical dashed line in the main frame. Main frame: Maximum pumped current for each contributing sub-band as a function of the driving frequency.  $eV_{ac}$  is set as in Fig. 1 and  $L = 100$  nm.

alternating hoppings  $\gamma_0$  and  $\gamma_q = 2\gamma_0 \cos(q\pi/N)$  ( $q = 0, 1, \dots, N-1$ ). When  $N$  is an integer multiple of three, the metallic subbands correspond to  $q = N/3$  and  $2N/3$ . Figure 2 shows the current pumped as a function of the gate voltage  $V_{gate}$  (inset) and driving frequency (main frame) applied to a (24,0) nanotube for a typical set of parameters. Different curves show the contributions coming from each subband with  $q = 7, 8$ , and  $9$  to the total current (since the contributions for  $q = 15, 16$ , and  $17$  are equal to those shown here, we concentrate only in the former). The curve labeled as  $q = 8$  corresponds to one of the two linear bands which crosses the CNP and which is responsible for the metallic character of the tube. The remaining curves,  $q = 7$  and  $q = 9$ , lead to the first and second van Hove singularities, respectively. By inspection of the inset, one sees that subbands labeled with  $q = 7$  and  $9$ , which reveal vHSs within the displayed gating range, dominate over the one with  $q = 8$ . Furthermore, the contributions due to  $q = 7$  and  $9$  reveal a maximum intensity close to the corresponding vHS and then a decay. What triggers such a dramatic increase of the current shown in Fig. 2 inset? Careful analysis of the numerical results shows that as the gate voltage is tuned closer to the vHS, there is a crossover from a regime where inelastic effects (which are responsible for non-adiabatic pumping) are weak to one where they become dominant (close to the vHS, where the level spacing becomes smaller than the driving frequency  $\hbar\Omega$ ).

Another relevant point is the scaling of the pumped current with the driving frequency. In contrast to adiabatic pumping, where the frequency can be made very small while keeping a constant pumped charge per cycle, for non-adiabatic pumping through a system with well separated resonances the frequency scaling of the pumped current is typically found to be quadratic.<sup>8,11,12</sup> In the main frame of Fig. 2, we show the frequency scaling of the maximum pumped current (discriminated by subband) in a broad range of frequencies going from tens of GHz to THz. Although, no simple behavior is expected for the maximum current due to a complicated interplay between finite size effects and driving parameters, Fig. 2 shows a dependence on frequency for  $q = 7$  and  $9$  which is for lower frequencies better than the quadratic one observed for  $q = 8$ . Notwithstanding, all the curves show a decrease for high enough frequency. This is shown only for  $q = 9$  in the plot where the current reveals a maximum value. This behavior can be understood as an interplay between the enhancement of inelastic processes for low frequency as the vHS becomes prominent and the opposite tendency produced when the frequency is large enough such that the field becomes ineffective in exciting photons. The same pumping behaviour was verified for armchair graphene nanoribbons, the only difference being the precise position of the vHS and the number of available channels.

In conclusion, most of the studies on quantum charge pumping focus on the behavior of a two-parameter pump close to isolated resonances. Here, we focused on a different scenario where non-adiabatic effects dominate: single-parameter pumping in a system with very good contacts. Our results are illustrated for two cases of much experimental relevance: carbon nanotubes and graphene nanoribbons. Besides offering currents that are higher than those driven close to the charge neutrality point, pumping phenomena held close to a van Hove singularity renders an improved scaling with frequency.

On the other hand, the pumped current close to the charge neutrality point may also be substantially enhanced by tuning the driving parameters and system size.

This work was supported by the Alexander von Humboldt Foundation, the European Union project CARDEQ under Contract No. IST-021285-2, SeCyT-UNC, CONICET (Argentina), and ANPCyT. G.C. acknowledges support from the South Korean Ministry of Education, Science, and Technology Program, Project WCU ITCE No. R31-2008-000-10100-0. Computing time provided by the ZIH at the Dresden University of Technology is also acknowledged.

- <sup>1</sup>D. J. Thouless, *Phys. Rev. B* **27**, 6083 (1983).
- <sup>2</sup>B. L. Altshuler and L. I. Glazman, *Science* **283**, 1864 (1999).
- <sup>3</sup>M. Büttiker and M. Moskalets, *Lect. Notes Phys.* **690**, 33 (2006).
- <sup>4</sup>M. Switkes, C. M. Marcus, K. Campman, and A. C. Gossard, *Science* **283**, 1905 (1999); F. Giazotto, P. Spathis, S. Roddaro, S. Biswas, F. Taddei, M. Governale, and L. Sorba, *Nat. Phys.* (2011), online only.
- <sup>5</sup>L. DiCarlo, C. M. Marcus, and J. S. Harris, Jr., *Phys. Rev. Lett.* **91**, 246804 (2003).
- <sup>6</sup>M. D. Blumenthal, B. Kaestner, L. Li, S. Giblin, T. J. B. M. Janssen, M. Pepper, D. Anderson, G. Jones, and D. A. Ritchie, *Nature Phys.* **3**, 343 (2007).
- <sup>7</sup>P. W. Brouwer, *Phys. Rev. B* **58**, R10135 (1998).
- <sup>8</sup>M. G. Vavilov, V. Ambegaokar, and I. L. Aleiner, *Phys. Rev. B* **63**, 195313 (2001).
- <sup>9</sup>M. Moskalets and M. Büttiker, *Phys. Rev. B* **66**, 205320 (2002).
- <sup>10</sup>L. Arrachea, *Phys. Rev. B* **72**, 121306(R) (2005).
- <sup>11</sup>L. E. F. Foa Torres, *Phys. Rev. B* **72**, 245339 (2005).
- <sup>12</sup>A. Agarwal and D. Sen, *Phys. Rev. B* **76**, 235316 (2007).
- <sup>13</sup>B. Kaestner, V. Kashcheyevs, S. Amakawa, M. D. Blumenthal, L. Li, T. J. B. M. Janssen, G. Hein, K. Pierz, T. Weimann, U. Siegner, and H. W. Schumacher, *Phys. Rev. B* **77**, 153301 (2008) *Appl. Phys. Lett.* **92**, 192106 (2008).
- <sup>14</sup>A. Fujiwara, K. Nishiguchi, and Y. Ono, *Appl. Phys. Lett.* **92**, 042102 (2008).
- <sup>15</sup>B. Kaestner, C. Leicht, V. Kashcheyevs, K. Pierz, U. Siegner, and H. W. Schumacher, *Appl. Phys. Lett.* **94**, 012106 (2009).
- <sup>16</sup>A. H. C. Neto, F. Guinea, N. M. R. Peres, K. S. Novoselov, and A. K. Geim, *Rev. Mod. Phys.* **81**, 109 (2009).
- <sup>17</sup>J.-C. Charlier, X. Blase, and S. Roche, *Rev. Mod. Phys.* **79**, 677 (2007); R. Saito, G. Dresselhaus, and M. S. Dresselhaus, *Physical Properties of Carbon Nanotubes* (Imperial College Press, London, 1998).
- <sup>18</sup>E. Prada, P. San-Jose, and H. Schomerus, *Phys. Rev. B* **80**, 245414 (2009).
- <sup>19</sup>R. Zhu and H. Chen, *Appl. Phys. Lett.* **95**, 122111 (2009).
- <sup>20</sup>R. P. Tiwari and M. Blaauw, *Appl. Phys. Lett.* **97**, 243112 (2010).
- <sup>21</sup>P. San-Jose, E. Prada, S. Kohler, and H. Schomerus, e-print arXiv:1103.5597.
- <sup>22</sup>Y. Gu, Y. H. Yang, J. Wang, and K. S. Chan, *J. Phys. Condens. Matter* **21**, 405301 (2009).
- <sup>23</sup>G. Li, A. Luican, J. M. B. Lopes dos Santos, A. H. C. Neto, A. Reina, J. Kong, and E. Y. Andrei, *Nature Phys.* **6**, 109 (2010).
- <sup>24</sup>S. Krompiewski, J. Martinek, and J. Barnas, *Phys. Rev. B* **66**, 073412 (2002).
- <sup>25</sup>Note that this ingredient, allowing for Fabry-Perot oscillations, is not present in Ref. 22.
- <sup>26</sup>W. Liang, M. Bockrath, D. Bozovic, J. H. Hafner, C. M. Lieber, M. Tinkham, and H. Park, *Nature* **411**, 665 (2001).
- <sup>27</sup>S. Camalet, J. Lehmann, S. Kohler, and P. Hänggi, *Phys. Rev. Lett.* **90**, 210602 (2003).
- <sup>28</sup>S. Kohler, J. Lehmann, and P. Hänggi, *Phys. Rep.* **406**, 379 (2005).
- <sup>29</sup>M. Guigou, A. Popoff, Th. Martin, and A. Crépieux, *Phys. Rev. B* **76**, 045104 (2007).
- <sup>30</sup>S. Roche, J. Jiang, L. E. F. Foa Torres, and R. Saito, *J. Phys.: Condens. Matter* **19**, 183203 (2007).
- <sup>31</sup>H. L. Calvo, H. M. Pastawski, S. Roche, and L. E. F. Foa Torres, *Appl. Phys. Lett.* **98**, 232103 (2011).
- <sup>32</sup>C. G. Rocha, L. E. F. Foa Torres, and G. Cuniberti, *Phys. Rev. B* **81**, 115435 (2010); C. G. Rocha, M. Pacheco, L.E.F. Foa Torres, G. Cuniberti, and A. Latge, *EPL* **94**, 47002 (2011).
- <sup>33</sup>L. E. F. Foa Torres and G. Cuniberti, *Appl. Phys. Lett.* **94**, 222103 (2009).
- <sup>34</sup>N. Mingo, L. Yang, J. Han, and M. P. Anantram, *Phys. Status Solidi B* **226**, 79 (2001).